Quasistatic interpretation of the He- and Ne-induced blue asymmetry of the 326.1-nm Cd line shapes in the core and near-wing regions

Ryszard S. Trawiński, Roman Ciuryło, and Józef Szudy
Instytut Fizyki, Uniwersytet Mikołaja Kopernika, ul. Grudziadzka 5/7, 87-100 Toruń, Poland
(Received 9 May 2006; published 15 August 2006)

A blue line shape asymmetry near the center of the Cd 326.1-nm line induced by low-polarizability perturbers (He, Ne) is explained by including the quasistatic contributions to the broadening rate associated with free-free transitions between repulsive branches of potential curves. The resulting shape in the near blue wing is represented by the addition to the Lorentzian and dispersion profiles of a quasistatic component. It is shown that for heavy perturbers (Ar, Kr, Xe) the quasistatic contributions play a marginal role near the line center and the line shape asymmetry arises mainly due to the finite duration of collision. It is also shown that for light perturbers (He, Ne) the quasistatic contributions are much more significant than those due to the collision duration and can adequately describe the blue asymmetry in the core region.

DOI: 10.1103/PhysRevA.74.022716 PACS number(s): 34.20.−b, 32.70.−n

I. INTRODUCTION

Much attention has been paid in the recent two decades to the asymmetries of pressure-broadened spectral line shapes observed at low perturber densities in the form of departures of the measured intensity distribution in the core and near-wing regions from the Voigt profile which is a convolution of Lorentzian and Gaussian distributions describing the collisional and Doppler components of the line shape, respectively [1–17]. These asymmetries were identified as coming from two distinct sources: (i) *a collision time asymmetry* from breakdown of the impact approximation [6–12] and (ii) *a collision correlation asymmetry* from the statistical dependence between pressure broadening and emitter velocity [13–17]. In the present paper we are concerned with pure pressure broadening only and the collision correlation effects are not considered. These effects, however, become increasingly apparent with increasing values of the ratio of the mass of perturber to emitter.

A pressure-induced asymmetry in the near-wing region results from the first-order correction to the Lorentzian distribution which has a *dispersion* shape in agreement with that derived first by Anderson and Talman [6] on the basis of the classical phase-shift theory and later by other researchers [7–12]. The term *collision time asymmetry* was first introduced by Harris *et al.* [2] because for van der Waals potentials the magnitude of the dispersion-shaped component was shown to be proportional to the collision duration. All these treatments predict that the asymmetry should be in the same direction as the pressure shift of the line. This means that a line with a redshift should have a more intense long-wavelength side (*red asymmetry*) whereas a *blueshift* should be associated with a *blue asymmetry*—i.e., a higher intensity in the short-wavelength side. Such a behavior has been confirmed experimentally for the cases of perturbation by heavier rare gases (Ar, Kr, Xe) of the sodium [1], calcium [2], strontium [3], and potassium [4] resonance lines. In all these cases both the redshift and red asymmetry were observed. On the other hand, Romalis *et al.* [5] observed the *blue asymmetry* and the *blueshift* for the D_1 and D_2 lines of rubidium perturbed by ^{4}He and ^{3}He isotopes. Contrary to that, for the cases of perturbation of the calcium resonance line (422.7 nm) by He and Ne, Harris *et al.* [2] have found that the shift (*red*) and asymmetry (*blue*) are in opposite directions. Similar results were obtained in our laboratory by Bielski *et al.* [16] who observed the redshift and blue asymmetry for the cadmium intercombination line (326.1 nm) perturbed by He and Ne.

The fact that the shift is towards the red indicates the dominant role of the attractive van der Waals potential in perturbations of the 422.7-nm calcium and 326.1-nm cadmium lines by helium and neon atoms. On the other hand, however, for this potential the dispersion-shaped correction to the Lorentzian profile calculated on the basis of treatments pioneered by Anderson and Talman [6–12] is such that it always yields the red asymmetry contrary to what is observed in experiments performed for Ca-He, Ca-Ne, Cd-He, and Cd-Ne. One of the reasons for such discrepancies between theory and experiment may, of course, be due to the assumed form of the interaction potential. Indeed, calculations performed by Bielski *et al.* [15] on the basis of *ab initio* potentials for Cd–rare-gas systems given by Czuchaj and Stoll [18] yielded the blueshift while the red one was observed in experiment. Moreover, for Cd-Ne the calculations based on the Czuchaj-Stoll potentials predicted the redshift (in qualitative agreement with experiment) and the red asymmetry in contradiction to experimental (*blue*) asymmetry. Such discrepancies seem to indicate that in some cases the dispersion-shaped correction to the Lorentzian profile connected with the collision-duration time is insufficient to interpret the observed asymmetry.

In the present work we shall focus our attention on the profiles of the intercombination ($5\,^3P_1$-$5\,^1S_0$) 326.1-nm cadmium line perturbed by rare-gas atoms for which precise measurements have recently been performed in our laboratory using the laser-induced fluorescence (LIF) method [15,16,19]. It is the main goal of this paper to show that the blue asymmetry of this line observed in cases of low-polarizability perturbers (He, Ne) can be explained by taking into account the contribution to the transition amplitude coming from the free-free transitions associated with the repulsive branches of potential curves. In the classical limit

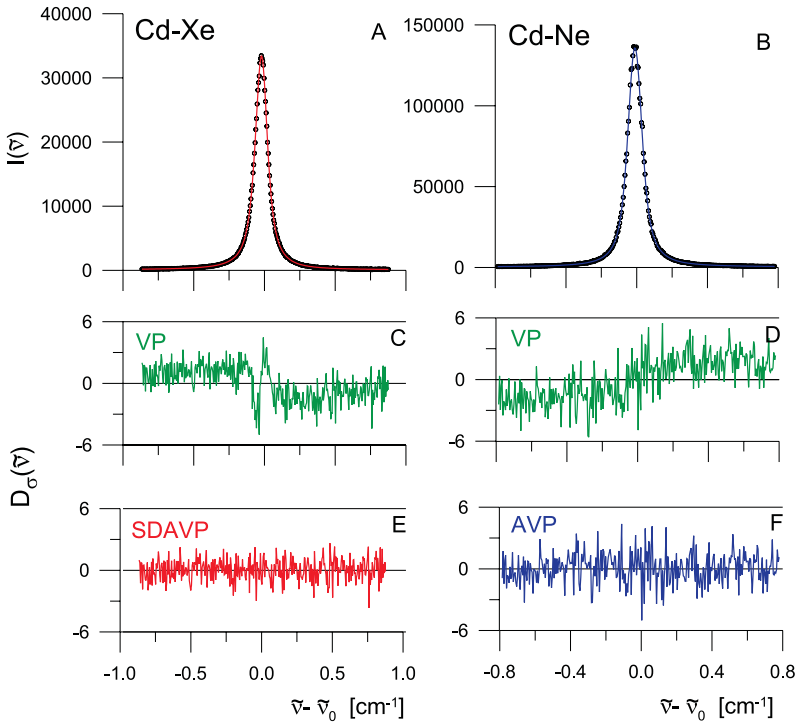

FIG. 1. (Color online) The shape of the ^{114}Cd 326.1-nm line perturbed by xenon at pressure 203 Torr and by neon at pressure 292 Torr: (A) and (B) experimental points together with the best-fit profiles (solid curves), (C) and (D) weighted differences $D_u(\tilde{\nu})$ between experimental points and fitted Voigt profiles (VP), and (E) and (F) weighted differences between experimental points and speed-dependent asymmetric Voigt profile (SDAVP) and asymmetric Voigt profile (AVP), respectively.

these contributions can be described in the framework of the quasistatic model. It will be shown that for perturbers with low values of polarizability they may contribute significantly to the intensity distribution even in the close neighborhood of the peak of the line in addition to both the Lorentzian and dispersion broadening and thus they can be regarded as an additional cause of asymmetry of a pressure-broadened spectral line in the core and near-wing regions superimposed on that due to the collision duration.

II. LINE SHAPE ASYMMETRY IN THE CORE AND NEAR-WING REGIONS

In order to avoid problems with overlapping hyperfine structure components associated with $5\,^3P_1$-$5\,^1S_0$ transition the ^{114}Cd isotope was used in measurements reported in Refs. [15,16,19]. This means that for this isotope the 326.1-nm line can be treated as a well-isolated line. For this reason in the present work we shall not deal with line-mixing effects, which in principle can also contribute to the asymmetry of the profile [20,21]. Our analysis is based on the unified Franck-Condon (UFC) formulation of the quasimolecular pressure broadening theory [7]. It is unified in the sense that on one hand in the *impact* limit valid for the core of the line it yields the Lorentzian shape with width [full width at half maximum (FWHM)] γ and the shift Δ identical to those resulting from the impact theory and on the other hand for far wings it yields the quasistatic profile. It should be emphasized, however, that the separation between impact and quasistatic (or core and far-wing) regions is relative to both the environment and the specific characteristics of a given line.

The Lorentzian profile is a characteristic feature of the *impact model* which assumes that the transition amplitudes are dominated by the region of very large interatomic separations $R(R\rightarrow\infty)$, and this permits us to express the width and shift parameters in terms of the scattering phase shifts for the upper and lower levels of the radiating atom in a close analogy to both quantum-mechanical and semiclassical formulas for the total cross section in elastic scattering of molecular beams. Beyond the *impact core*—i.e., for frequencies in the far wings which correspond to smaller values of R—the impact approximation fails completely and, in particular, it cannot explain the origin of the so-called *rainbow* satellite bands which may appear in the form of diffuse maxima on line wings. It was shown [7,22–26] that such satellites arise whenever the difference $\Delta V(R)=V'(R)-V''(R)$ of interatomic potentials $V'(R)$ and $V''(R)$ for the upper and lower levels of the radiating atom, respectively, has an extremum. This represents an analogy with the famous *rainbow effect* in the elastic scattering which takes place when the classical deflection function possesses an extremum [27–29]. Although the possibility of the formation of rainbow satellites in the core and near-wing regions cannot be, in principle, excluded from consideration, usually they were experimentally detected for many atomic systems at far line wings [7,23–26]. Since in the present work we are concerned with the profiles in the line core and near wings, the rainbow effects will not be discussed here.

The use of the LIF method in our recent studies on the Cd–rare-gas-atom systems [15,16,19] and, in particular, the high resolution, high signal to noise ratio, and negligible instrumental function enabled us to record deviations of the experimental profiles from the ordinary Voigt profile (VP) which represents a convolution of the Lorentzian and Doppler profiles. Two examples of experimental profiles of the 326.1-nm ^{114}Cd line are shown in Fig. 1(a) for the case of perturbation by Xe at pressure 203 Torr (temperature T

=724 K), and in Fig. 1(b) for perturbation by Ne at pressure 292 Torr (T=724 K). The evidence that our experimental profiles are asymmetric is demonstrated in Fig. 1(c) for Cd-Xe and in Fig. 1(d) for Cd-Ne, where we have plotted the residuals representing the weighted differences between the experimental shape and the ordinary VP used to fit the data. In both Figs. 1(c) and 1(d) we can see systematic departures of residuals from zero that be regarded as a manifestation of the line asymmetry. The plots in Figs. 1(c) and 1(d) clearly indicate *red* asymmetry for Cd-Xe and *blue* asymmetry for Cd-Ne. The *blue* asymmetry was also found for the 326.1-nm ^{114}Cd line perturbed by He while the *red* asymmetry apart from Xe was also observed for the cases of perturbation by Ar and Kr [15,16,19].

A careful analysis performed in Refs. [15,16] showed that for Cd-Ne and Cd-He the experimental profiles can be fitted well to the asymmetric Voigt profile (AVP) which represents convolution of the Doppler distribution with a sum of the Lorentzian and dispersion profiles. Figure 1(f) shows the plots of weighted differences between the experimental profile and the AVP for Cd-Ne. It is seen that the differences are spread uniformly about zero which confirms the good quality of the AVP fit. We should note, however, that as was reported in Ref. [19] for Cd-Xe the experimental profiles cannot be fitted sufficiently well to AVP due to the large value of the mass of the Xe atom. The best fit in this case was obtained for the speed-dependent asymmetric Voigt profile (SDAVP) which accounts for the correlation between the Doppler and pressure broadening. The good quality of the SDAVP fit for Cd-Xe is demonstrated by the uniform spread of residuals in Fig. 1(e). The main conclusion which can be drawn from studies reported in Ref. [19] is that in case of perturbation by a heavy atom such as Xe characterized by a large value of the polarizability the inclusion of speed-dependent effects and the finite duration of collision is sufficient to interpret the observed *red* asymmetry on the basis of a purely attractive van der Waals potential. That is not the case for the broadening by low-polarizability atoms such as He and Ne for which speed-dependent effects play a marginal role while the theoretical collision duration asymmetry is much smaller than that observed in experiment.

III. UNIFIED QUASIMOLECULAR MODEL

We start with the UFC formula for the intensity distribution $I(\xi)$ in the pressure broadened line—namely [7],

$$I(\xi) = \frac{1}{\pi}\frac{N\Gamma(\xi)}{\xi^2 + (\gamma/2)^2}, \tag{1}$$

where N is the density number of perturbers, ξ is the frequency displacement from the impact-shifted line center,

$$\xi = \omega - \omega_0 - \Delta, \tag{2}$$

and ω_0 is the unperturbed frequency of the line. In Eq. (1), $\Gamma(\xi)$ is the frequency-dependent pressure-broadening rate which can be expressed in terms of the free-free Franck-Condon factors, or squares of overlap integrals $H_l(\xi)$, in the following way:

$$\Gamma(\xi) = \left\langle \frac{\pi\hbar}{\mu k_i}\sum_{l=0}^{\infty}(2l+1)|H_l(\xi)|^2 \right\rangle. \tag{3}$$

Here l is the orbital quantum number of the relative motion, μ is the reduced mass of the radiating and perturbing atoms, and the symbol $\langle\cdots\rangle$ indicates the average over initial wave vectors k_i, or initial energies $E_i=\hbar^2k_i^2/2\mu$. In Eq. (3), $H_l(\xi)$ is given by

$$H_l(\xi) = \sqrt{2}\pi\hbar\xi\mathcal{A}_l(\xi), \tag{4}$$

where

$$\mathcal{A}_l(\xi) = \int_0^{\infty}\Psi_i^{(l)}(R)\Psi_f^{(l)}(R)dR \tag{5}$$

is the overlap integral of the energy-normalized radial wave functions $\Psi_i^{(l)}(R)$ and $\Psi_f^{(l)}(R)$ of the perturber with angular momentum l for the initial (i) and final (f) levels of the radiating atom, respectively (R is the separation between radiating and perturbing atoms).

The traditional analysis of the intensity distribution in the core region corresponding to small values ξ of frequency displacements assumes the validity of the *impact approximation* in which the collisions are treated as instantaneous so that the collision duration time is assumed to be negligibly short. This is equivalent to the assumption that the essential contribution to the overlap integral in Eq. (5) comes from the encounter of the radiating atoms with the perturbers which are incident at very large interatomic separations ($R\to\infty$). Such perturbers are only slightly deflected by the tail of the interaction potential $V_i(R)$ in the initial state so that their *local wave number* $k_l(R)$,

$$k_l(R) = \left\{\frac{2\mu}{\hbar^2}[E_i - V_i(R)] - \frac{l(l+1)}{R^2}\right\}^{1/2}, \tag{6}$$

can be replaced by the free motion wave number $k_i=k_l(\infty)$ and the overlap integral $H_l(\xi)$ may then be evaluated assuming the radial wave functions in Eq. (5) to be given by their asymptotic forms for ($R\to\infty$). Thus in the impact limit one obtains [7]

$$H_l(\xi) \approx H_l^{(\infty)} = \sqrt{2}\sin[\delta_l' - \delta_l''], \tag{7}$$

where δ_l' and δ_l'' are the scattering phase shifts for the upper and lower levels of the radiating atom, respectively. After substitution into Eq. (3) we obtain, for the *impact* pressure-broadening rate,

$$\Gamma(\xi) \approx \Gamma^{(\infty)} = \frac{\beta}{2} = \left\langle \frac{2\pi\hbar}{\mu k_i}\sum_{l=0}^{\infty}(2l+1)\sin^2[\delta_l' - \delta_l''] \right\rangle, \tag{8}$$

where $\beta=\gamma/N$ is the pressure-broadening coefficient. The resulting line shape, Eq. (1), has then the Lorentzian form

$$I_L(\xi) = \frac{\gamma}{2\pi}\frac{1}{\xi^2 + (\gamma/2)^2}, \tag{9}$$

as predicted first by Sobelman [30] and Baranger [31] in their quantum-mechanical impact theory.

To improve upon the Lorentzian shape the overlap integral in Eq. (5) can be evaluated using the JWKB wave functions and for small ξ an expansion of $H_l(\xi)$ in powers of ξ can be made following Ref. [7]:

$$H_l^{(\infty)}(\xi) = \sqrt{2}\sin[\delta_l' - \delta_l''] + \sqrt{2}\xi a_l, \tag{10}$$

where a_l is the frequency-independent factor which in the classical-path approximation can be expressed as a function $a_l = a(b)$ of the impact parameter b in the following way [7]:

$$a(b) = \frac{1}{\hbar}\int_0^\infty dt \Delta V(R(t))t \sin\left[\frac{1}{\hbar}\int_0^t \Delta V(R(t'))dt'\right]. \tag{11}$$

Here the interatomic distance $R = R(t) = (b^2 + v^2t^2)^{1/2}$ is expressed as a function of time t and the impact parameter, and $v = \hbar k_i/\mu$ is the initial velocity. Deriving Eq. (11) we have replaced the sum over angular momenta l by an integral over b. Equation (3) yields then, for the asymptotic pressure-broadening rate,

$$\Gamma(\xi) \approx \Gamma^{(\infty)}(\xi) = \frac{\beta}{2} + \kappa\xi, \tag{12}$$

where the coefficient κ can be calculated using an expression derived in Ref. [7]:

$$\kappa = \left\langle 8\pi v \int_0^\infty ba(b)\sin[\delta'(b) - \delta''(b)]db \right\rangle, \tag{13}$$

where $\delta_l' = \delta'(b)$ and $\delta_l'' = \delta''(b)$ are the scattering phase shifts for the upper and lower levels of the radiating atom, respectively, expressed as functions of the impact parameter b. In Eq. (11) the difference potential $\Delta V(R(t)) = V'(R(t)) - V''(R(t))$ depends on both t and b. By substitution of Eq. (12) into Eq. (1) we obtain an asymmetric line shape

$$I(\xi) \approx I_{CD}(\xi) = \frac{1}{\pi}\frac{\gamma/2 + N\kappa\xi}{\xi^2 + (\gamma/2)^2}, \tag{14}$$

which is the sum of the Lorentzian and dispersion profiles. It describes the intensity distribution in the core and near-wing regions on both the *red* ($\xi < 0$) and *blue* ($\xi > 0$) side of the line. Following Kristensen *et al.* [32] the profile $I_{CD}(\xi)$ will be referred to as the *asymmetric Lorentzian* profile. The magnitude κ in Eq. (14) can be regarded as a measure of the line shape asymmetry, and for the van der Waals potentials it can be expressed in terms of the *collision duration* (CD) time and therefore κ is usually referred to as the *collision-time asymmetry coefficient* [2,7–12,15,16,19]. It should be noted that the sign of κ calculated on the basis of Eq. (12) is the same as the sign of the pressure shift (Δ) of the line calculated in the framework of the impact approximation.

As seen from Eqs. (11) and (13) a crucial role in the production of the line shape asymmetry is played by the function $\Delta V(R)$ describing the dependence of the potential difference upon the interatomic separation R. In many cases a curve representing $\Delta V(R)$ looks like the plot shown in Fig. 2. The intensity distribution given by Eq. (14) is valid for small values ξ—i.e., in the core of the line—and is produced

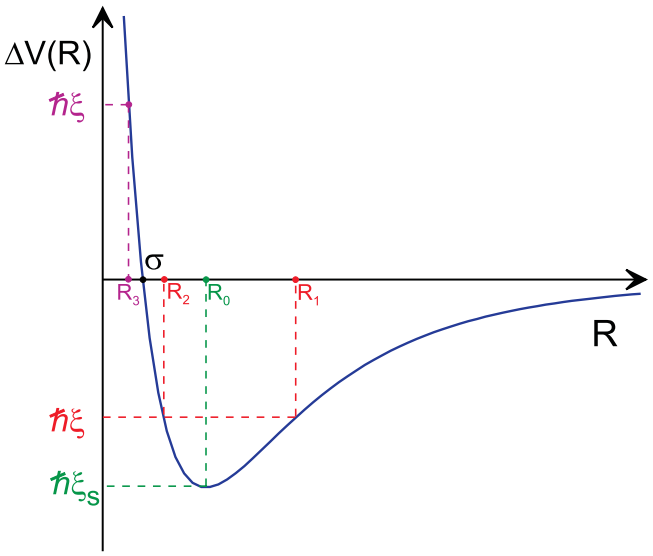

FIG. 2. (Color online) Plot of the difference potential $\Delta V(R)$. Notations explained in the text.

by those phase shifts, averaged over impact parameters, which are dominated by the interaction potentials at very large separations ($R \to \infty$) leading to small perturbations of the atomic states. Contrary to that, the large values ξ of the frequency displacement located on the far line wings correspond to large perturbations of the upper and lower states of the radiating atom caused by its interaction with the perturber at small separations R. As noted first by Jabłoński [33], who used the JWKB wave functions, the dominant contribution to the overlap integral $H_l(\xi)$ for large ξ comes from the region of stationary phase—i.e., from the region of R situated in the vicinity of Condon points R_c defined as solutions of the equation

$$\hbar\xi = \Delta V(R_c), \tag{15}$$

which permits us to express ξ as a function of the interatomic separation R. This means that the negative region [$\xi = \Delta V(R)/\hbar < 0$] of the plot shown in Fig. 2 which is associated with predominance of the attraction corresponds to the red wing of the line, whereas the positive region associated with domination of the repulsive interactions corresponds to the blue wing ($\xi > 0$). We should note that in the case of difference potentials of the type shown in Fig. 1 for a given value ξ of the frequency displacement located on the red side of the line there are two Condon points associated with attractive forces: the *outermost attractive* Condon point R_1 and the *inner attractive* Condon point R_2. Contrary to that, for the blue side there is only one Condon point R_3 to be referred to as the *inner repulsive* Condon point because it corresponds to the repulsive branch of $\Delta V(R)$. If R_1 and R_2 are very close each other—i.e., in the neighborhood of the interatomic separation R_0 at which $\Delta V(R)$ has a minimum—the overlap integral in Eq. (5) can be evaluated by the method of Sando and Wormhoudt [22] used to calculate the shape of the *rainbow* satellite bands associated with extrema of difference potentials [7,22–25] in an analogy to the Ford-Wheeler theory

of rainbow scattering [27–29]. In the case when $\Delta V(R)$ has a minimum in the attractive region ($\xi<0$) as in Fig. 2, the rainbow satellite is located on the red wing of the line at the frequency $\xi_s=-\varepsilon$ with respect to the line peak, where ε denotes the depth of the attractive well of $\Delta V(R)$. The main features of the rainbow satellites seem to be well understood [7,22–26], and we are not concerned with them here. In the present work we are dealing with the core and very-near-wing regions of the line only, so our discussion will be restricted to small values of ξ.

The interpretations of all experimental studies on asymmetry of atomic spectral line shapes performed in the last years employed the asymmetric Lorentzian, Eq. (14), in which the non-Lorentzian behavior in the core region was related to the collision-time asymmetry. It should be emphasized that Eq. (14) itself can be related to the Fourier transform of the asymptotic form of the correlation function in the scattering limit and is applicable in the central part of the line both on the red ($\xi<0$) and blue ($\xi>0$) sides of the line. In the following section we shall show that in some cases, especially those for which the repulsive interactions are strong enough, the transitions between repulsive branches of potential curves that give rise to positive values of frequency displacement may significantly contribute to the overlap integral in the blue side of the line even for very small ξ. As indicated in Fig. 2 it may happen for such transitions that the inner repulsive Condon point R_3 is near the classical turning point R_t of the initial state defined as such value of interatomic separation for which the local wave number in Eq. (6) vanishes: $k_l(R_t)=0$.

Let $H_l^{(3)}(\xi)$ denote the contribution to the overlap integral coming from the transitions that occur near $R_3\approx R_t$. The total overlap integral $H_l(\xi)$ for $\xi>0$ can thus be written approximately as the sum of $H_l^{(3)}(\xi)$ and the asymptotic *extended impact* term $H_l^{(\infty)}(\xi)$:

$$H_l(\xi)\approx H_l^{(3)}(\xi)+H_l^{(\infty)}(\xi), \tag{16}$$

where $H_l^{(\infty)}(\xi)$ is given by Eq. (10). With this $H_l(\xi)$ one obtains from Eq. (3) the following formula for the broadening rate on the blue side of the line for small ξ:

$$\Gamma(\xi)=\left\langle \frac{\pi\hbar}{\mu k_i}\sum_{l=0}^{\infty}(2l+1)|H_l^{(3)}(\xi)+H_l^{(\infty)}(\xi)|^2\right\rangle$$
$$=\Gamma^{(\infty)}(\xi)+\Gamma^{(3)}(\xi)+\Gamma^{(3,\infty)}(\xi), \tag{17}$$

where

$$\Gamma^{(3)}(\xi)=\left\langle \frac{\pi\hbar}{\mu k_i}\sum_{l=0}^{\infty}(2l+1)|H_l^{(3)}(\xi)|^2\right\rangle \tag{18}$$

is the broadening rate associated with the inner repulsive Condon point R_3, $\Gamma^{(\infty)}(\xi)$ is given by Eq. (12), and

$$\Gamma^{(3,\infty)}(\xi)=\left\langle \frac{2\pi\hbar}{\mu k_i}\sum_{l=0}^{\infty}(2l+1)|H_l^{(3)}(\xi)H_l^{(\infty)}(\xi)|\right\rangle \tag{19}$$

is an interference term which accounts for contributions due to interference between transition amplitudes associated with inner repulsive Condon points R_3 and those related to the scattering effects that occur at very large interatomic separations ($R\to\infty$). This term is difficult to evaluate numerically. One can expect, however, that its contribution to the resulting broadening rate is negligible, and therefore in the following section this term will be omitted.

IV. QUASISTATIC BROADENING IN THE NEAR BLUE WING

The JWKB wave functions used in Ref. [7] to derive the *asymmetric Lorentzian* formula for the broadening rate, Eq. (12), fail when Condon points are near the classical turning points because their amplitude becomes infinite in the vicinity of R_t. To overcome this difficulty Bieniek [34] proposed to use the uniform JWKB wave functions expressed in terms of homogeneous Airy functions in such a way that for $R\approx R_t$ they attain the form of the exact solution of the Schrödinger equation and for $R\gg R_t$ they become identical to the ordinary JWKB wave functions. In Ref. [35] the uniform JWKB wave functions were applied to evaluate the overlap integrals $H_l^{(3)}(\xi)$, Eq. (5), associated with the inner repulsive Condon points R_3, producing positive frequency displacements ($\xi>0$) as a result of transitions between repulsive branches of potential curves. It was shown that $H_l^{(3)}(\xi)$ can be written in the form of a sum of a *nonclassical* term describing contributions due to effects originated in the classically inaccessible region ($R<R_t$) and a term which accounts for the contributions to the overlap integral coming from the classically accessible region ($R>R_t$). Since the nonclassical term was shown to be given by the Airy function of the positive argument, it is expected to decay exponentially and therefore its role in most cases is negligible. If this term is ignored, then $H_l^{(3)}(\xi)$ can be approximately written in the form resulting from the Jabłoński [33] derivation based on the ordinary JWKB wave functions:

$$H_l^{(3)}(\xi)=2\xi\left[\frac{\pi\mu}{|k_l(R_3)|}\right]^{1/2}\cos[\Phi_l(R_3)]\left|\frac{d\Delta V(R)}{dR}\right|_{R_3}^{-1/2}, \tag{20}$$

where $\Phi_l(R_3)$ is the phase-shift difference at R_3 between upper and lower states. As indicated by Mies [36] the cosine factor may be responsible for quantum oscillations which, however, tend to vanish after the thermal averaging is performed. Combining Eqs. (20) and (18), making use of the random phase approximation with $2\cos^2\Phi_l(R_3)=1$, and performing the Maxwellian averaging over initial wave vectors k_i one obtains for the broadening rate $\Gamma_3(\xi)$ associated with repulsive branches of potential curves the following expression:

$$\Gamma^{(3)}(\xi)=4\pi^2\hbar R_3^2\left|\frac{d\Delta V(R)}{dR}\right|_{R_3}^{-1}\xi^2\exp\left(-\frac{V_i(R_3)}{k_BT}\right), \tag{21}$$

where k_B is the Boltzmann constant. Hereafter the broadening rate $\Gamma_3(\xi)$ given by Eq. (21) will be referred to as the *quasistatic broadening rate* since it can be derived directly in the framework of the quasistatic model [7,23,37]. To derive

Eq. (21) we have replaced the sum in Eq. (18) by an integral over l. Traditionally the quasistatic theory was used to interpret the shapes of far wings of the line [23,37]. Nevertheless, we shall show in the following section that quasistatic contributions can at times be significant also in the central part of the line on its blue side.

In order to estimate the influence of quasistatic broadening rate $\Gamma^{(3)}(\xi)$ associated with repulsive branches of potential curves on the intensity distribution in the core region let us describe the difference potential $\Delta V(R)$ by the Lennard-Jones model potential

$$\Delta V(R) = \hbar\left[\frac{\Delta C_{12}}{R^{12}} - \frac{\Delta C_6}{R^6}\right] \tag{22}$$

or

$$\Delta V(R) = 4\varepsilon\hbar\left[\left(\frac{\sigma}{R}\right)^{12} - \left(\frac{\sigma}{R}\right)^{6}\right], \tag{23}$$

where $\Delta C_{12}=4\varepsilon\sigma^{12}$ and $\Delta C_6=4\varepsilon\sigma^6$. For $R=\sigma$ we have $\Delta V(\sigma)=0$ and $\xi=0$. The Lennard-Jones potential is used in this paper to illustrate the procedure, but the method is applicable to any potential. For the blue side ($\xi>0$) of the line there is only one root of Eq. (15), which is only the *inner repulsive* Condon point R_3 given by

$$R_3 = \left[\frac{2\varepsilon}{\xi}\right]^{1/6}\sigma\left[\sqrt{1+\frac{\xi}{\varepsilon}} - 1\right]^{1/6}. \tag{24}$$

Let us note that for $\xi\to 0$ we have $R_3\to\sigma$. Substitution of the above expressions into Eq. (21) yields the following formula for the *quasistatic* broadening rate for the *blue* side:

$$\Gamma^{(3)}(\xi) = \frac{\pi^2}{6}\sqrt{2\Delta C_6\xi}f(\xi)\exp\left[-\frac{V_i(R_3)}{k_BT}\right], \tag{25}$$

where the function $f(\xi)$ is given by

$$f(\xi) = \frac{[\sqrt{1+\xi/\varepsilon}-1]^{3/2}}{\sqrt{1+\xi/\varepsilon}}. \tag{26}$$

Let us note that in the limit $\xi\to 0$ we have $f(\xi)\to 0$. This means that in the limit $\xi\to 0$ the *quasistatic broadening rate* $\Gamma^{(3)}(\xi)\to 0$ and the intensity in the peak of the line becomes equal to $I(0)=2/\pi\gamma$ in full accordance with that resulting from the *purely impact*—i.e., the Lorentzian line shape. Combining Eqs. (12), (17), and (25) we obtain the following formula for the resulting broadening rate on the blue side of the line ($\xi>0$):

$$\Gamma_{blue}(\xi) = \frac{\beta}{2} + \kappa\xi + \Gamma_3(\xi) = \frac{\beta}{2} + \kappa\xi + \frac{\pi^2}{6}\sqrt{2\Delta C_6\xi}f(\xi), \tag{27}$$

where we have assumed that $V_i(R_3)\ll k_BT$. Substitution of Eq. (27) into Eq. (1) yields for the intensity distribution $I_{blue}(\xi)$ in the *near blue wing* the following formula:

$$I_{blue}(\xi) = I_{CD}(\xi) + I_{QS}(\xi), \tag{28}$$

where $I_{CD}(\xi)$ is the asymmetric Lorentzian, Eq. (14), and

TABLE I. The values of $\hbar\Delta C_6$ (in units 10^{-67} J cm^6) and $\hbar\Delta C_{12}$ (in units 10^{-109} J cm^{12}) force constants of the Lennard-Jones potential.

	$\hbar\Delta C_6$	$\hbar\Delta C_{12}$	$\hbar\varepsilon$ [cm^{-1}]	σ [nm]
Cd-He	10.22	0.33	0.40	0.564
Cd-Ne	19.78	0.59	0.835	0.557
Cd-Ar	82.07	1.67	5.08	0.522
Cd-Kr	122.39	2.50	7.54	0.523
Cd-Xe	202.15	4.27	12.05	0.526

$$I_{QS}(\xi) = \frac{N\pi}{6}\frac{\sqrt{2\Delta C_6\xi}f(\xi)}{\xi^2 + (\gamma/2)^2} \tag{29}$$

is the quasistatic profile. It should be noted that for frequencies located at the extreme far blue wing such that $\xi/\varepsilon\gg 1$ the function $f(\xi)$ behaves like $\xi^{1/4}$ and then $I_{QS}(\xi)\sim\xi^{-5/4}$ in accordance with the quasistatic shape resulting from Eq. (21) for the purely repulsive potential $\sim R^{-12}$. On the red side of the line the total broadening rate $\Gamma_{red}(\xi)$ is

$$\Gamma_{red}(\xi) = \frac{\beta}{2} + \kappa\xi, \tag{30}$$

so that according to Eq. (1) the resulting intensity distribution $I_{red}(\xi)$ on the near red wing is simply identical to the asymmetric Lorentzian:

$$I_{red}(\xi) = I_{CD}(\xi), \tag{31}$$

As seen from Eqs. (28) and (31), $\Gamma^{(3)}(\xi)$ leads to an increase of the intensity on the blue side in comparison to that on the red one. This means that the *quasistatic* broadening rate gives rise to an additional asymmetry on the blue side which is superimposed on the collision-time asymmetry.

V. ASYMMETRY FACTORS FOR THE CADMIUM INTERCOMBINATION LINE PERTURBED BY RARE GASES

In order to estimate the role of the *quasistatic* contributions in the formation of asymmetric line shapes in the core region we have calculated the asymmetry factors for the case of the Cd intercombination 326.1-nm-line ($5\,^3P_1$-$5\,^1S_0$) perturbed by rare gases. We have modeled the difference potential $\Delta V(R)$ for the Cd+rare-gas-atom systems by the Lennard-Jones function, Eq. (23). The values of the constants ΔC_6, ΔC_{12}, σ, and ε calculated using a method due to Hindmarsh *et al.* [38] are listed in Table I.

It is seen that the depths ε of the difference potentials for Cd-He and Cd-Ne are much smaller that those for Cd-Ar, Cd-Kr, and Cd-Xe. In their experiments on the effects caused by He and Ne on the 326.1-nm Cd intercombination line Bielski *et al.* [16] have found the *blue* asymmetry but the *redshift* ($\Delta<0$) of this line both for perturbation by He and by Ne. The experimental values of the pressure broadening (β) and pressure shift ($\delta=\Delta/N$) coefficients as well as the *collision-time asymmetry* coefficient κ determined in Ref.

TABLE II. The values of the pressure broadening β, shift δ [in units 10^{-20} $cm^{-1}/(atom\ cm^{-3})$] and asymmetry κ [in units $10^{-21}/(atom\ cm^{-3})$] coefficients of the 326.1-nm ^{114}Cd line calculated (Calc.) for the Lennard-Jones potential together with experimental (Expt.) values. Numbers in parentheses are the values of standard uncertainty.

	Expt.			Calc.		
Perturber	β	δ	κ	β	δ	κ
Cd-He	1.155	−0.031	0.62	1.046	0.047	0.086
	(0.034)	(0.009)	(0.34)			
Cd-Ne	0.715	−0.090	0.17	0.735	−0.062	0.065
	(0.004)	(0.005)	(0.07)			
Cd-Ar	1.060	−0.387	−0.30	0.933	−0.474	−0.383
	(0.006)	(0.004)	(0.05)			
Cd-Kr	1.147	−0.338	−1.00	1.169	−0.536	−1.054
	(0.011)	(0.005)	(0.07)			
Cd-Xe	1.257	−0.348	−1.08	1.488	−0.547	−1.94
	(0.006)	(0.002)	(0.07)			

[16] are listed in Table II, where they are compared with theoretical values calculated on the basis of the Lennard-Jones potential with force constants given in Table I.

Theoretical values of β and δ are calculated in the framework of the Lindholm-Foley classical impact theory using a formalism due to Hindmarsh *et al.* [38]. The values of the collision-time asymmetry coefficient κ were calculated from Eq. (13). As seen from Table II both for Cd-He and Cd-Ne the calculations yielded the blue asymmetry ($\kappa>0$). On the other hand, for Cd-Ne the calculated shift is towards the red ($\delta<0$), in agreement with experiment, but for Cd-He the calculated shift is towards the blue ($\delta>0$) while the red one was observed [16].

The absolute values of both the experimental and calculated pressure shift coefficients are very small, and this fact seems to corroborate a suggestion that for Cd-He and Cd-Ne repulsion effects may play a crucial role. Following this suggestion we have performed calculations of the profiles of the 326.1-nm Cd line perturbed by all rare gases using Eqs. (28) and (31) with the Lennard-Jones force constants listed in Table I. Two examples of calculated profiles are shown in Fig. 3 for Cd-Ne (at neon pressure 440 Torr) and in Fig. 4 for Cd-Xe (at pressure 440 Torr). The differences between $I_{blue}(\xi)$ or $I_{red}(\xi)$ and the Lorentzian profile which are also plotted in Figs. 3 and 4 clearly demonstrate the importance of the quasistatic contribution on the blue side for the case of broadening by Ne. Similar results were obtained for Cd-He. Contrary to that seen in Fig. 4, for Cd-Xe the quasistatic contributions play a completely negligible role in the core region. Identical results were obtained for Cd-Ar and Cd-Kr. It should be noted, however, that for heavy perturbers such as Ar, Kr, and Xe the quasistatic contributions are dominant at extreme far wings which are not considered here.

Let us define now the frequency-dependent asymmetry factor $A(\xi)$ as

$$A(\xi) = \frac{I(\xi) - I_L(\xi)}{I_L(\xi)}, \tag{32}$$

where $I_L(\xi)$ denotes the Lorentzian profile, Eq. (9).

In the case when only the dispersion correction due to the effect of *collision duration* is taken into account the line total shape $I(\xi)$ can be approximated by the asymmetric Lorentzian profile $I_{CD}(\xi)$ given by Eq. (14) and then the collision-time asymmetry factor $A(\xi)=A_{CD}(\xi)$ can be written as

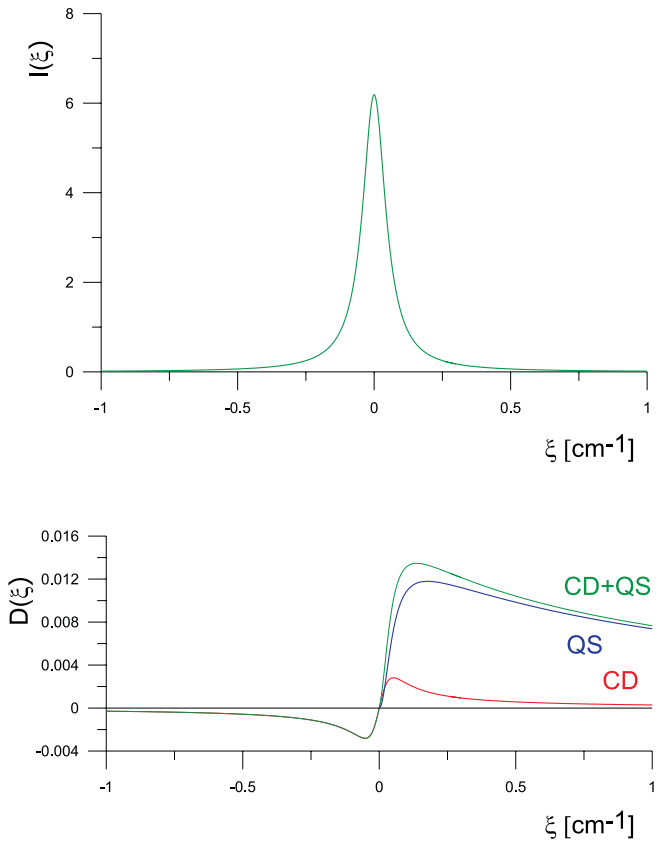

FIG. 3. (Color online) Plots of the calculated profile $I(\xi)$ for the 326.1-nm Cd line perturbed by neon at pressure 440 Torr together with the $D(\xi)$ differences between $I_{blue}(\xi)$ or $I_{red}(\xi)$ and the Lorentzian profile.

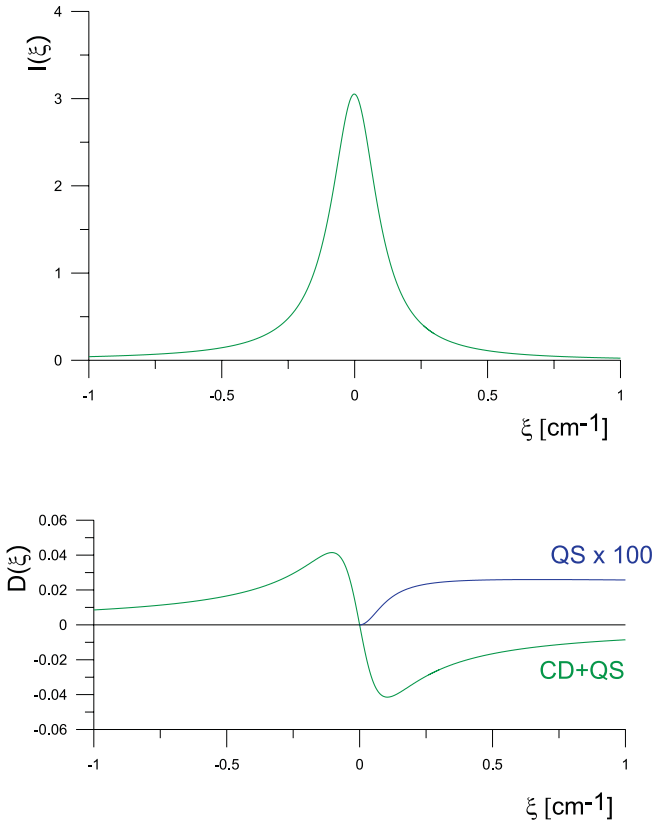

FIG. 4. (Color online) Plots of the calculated profile $I(\xi)$ for the 326.1-nm Cd line perturbed by xenon at pressure 440 Torr together with the $D(\xi)$ differences between $I_{blue}(\xi)$ or $I_{red}(\xi)$ and the Lorentzian profile.

$$A_{CD}(\xi) = \frac{2}{\beta}\kappa\xi. \tag{33}$$

This means that in this case the asymmetry factor is linearly dependent on the frequency displacement ξ. Equation (33) is applicable both on the *red* and *blue* sides of the line. However, for the red side the collision-duration effect is, in the model assumed in this work, the only cause of the asymmetry and thus the total asymmetry factor $A_{red}(\xi)$ on the *red* side is

$$A_{red}(\xi) = A_{CD}(\xi). \tag{34}$$

On the *blue* side of the line the total profile is given by Eq. (28) so that the resulting asymmetry factor for $\xi > 0$ may be written as

$$A_{blue}(\xi) = A_{CD}(\xi) + A_{QS}(\xi), \tag{35}$$

where

$$A_{QS}(\xi) = \frac{2\pi^2}{6\beta}\sqrt{2\Delta C_6 \xi} f(\xi) \tag{36}$$

is the *quasistatic asymmetry factor*.

Using the force constants from Table I we have calculated the quasistatic asymmetry factors $A_{QS}(\xi)$ for the *blue* side of the 326.1-nm Cd line perturbed by all rare gases. The results of these calculations are plotted in Fig. 5 for frequency displacements ξ up to 0.5 cm^{-1} from the maximum of the Cd intercombination line. As can be seen the quasistatic asymmetry factor increases with decreasing values of the polarizability of the perturbing atom. In particular, the quasistatic contribution to the asymmetry appears to be very large for light perturbers (He and Ne) characterized by small values of the polarizability. In order to get more insight into the problem of the influence of quasistatic effects on the production of line shape asymmetry in the core region in Figs. 6 and 7 we have plotted the total asymmetry factors (CD+QS) calculated from Eq. (35) as well as *collision-time asymmetry factors* $A_{CD}(\xi)$ for the *red* ($\xi < 0$) and the *blue* ($\xi > 0$) sides of the 326.1-nm line and the *quasistatic asymmetry factors* $A_{QS}(\xi)$ for the blue side of this line perturbed by Ne and Xe. In case of broadening by He the plots are similar to those in Fig. 6 while for Ar and Kr they are similar to those shown in Fig. 7.

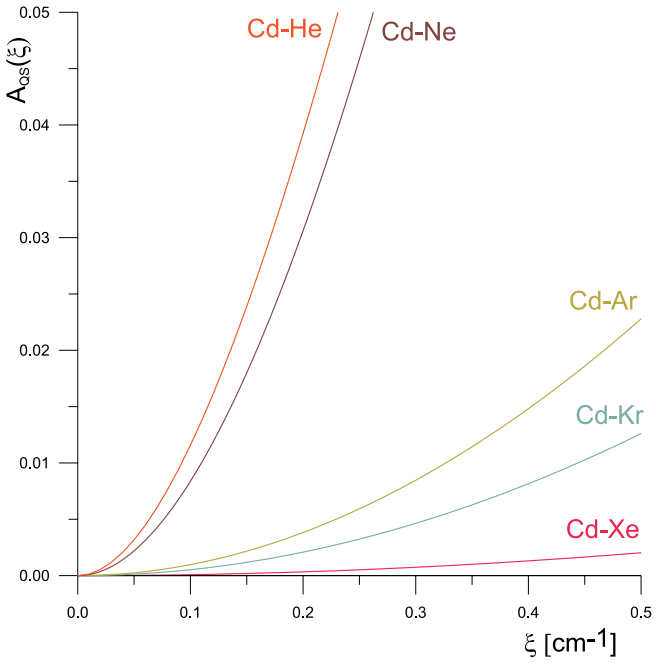

FIG. 5. (Color online) Quasistatic asymmetry factors $A_{QS}(\xi)$ for the blue side of the 326.1-nm Cd line perturbed by all rare gases.

VI. CONCLUSION

The comparison with experimental asymmetry factors determined on the basis of measurements reported in Refs. [15,16] shows that for Cd-He and Cd-Ne the inclusion of quasistatic broadening effects is necessary to explain the *blue* asymmetry induced by low-polarizability perturbers for which the transitions associated with repulsive parts of potential curves play a dominant role. Traditionally, such transitions have been taken into account to interpret the intensity distribution for very large positive frequency displacements ξ situated at the *far blue wing* of the line. Figures 5–7 indicate, however, that in the case of a perturbation by He and Ne they may also be important for very small frequency displacements ξ lying in the *near-blue-wing* and *core* regions of the

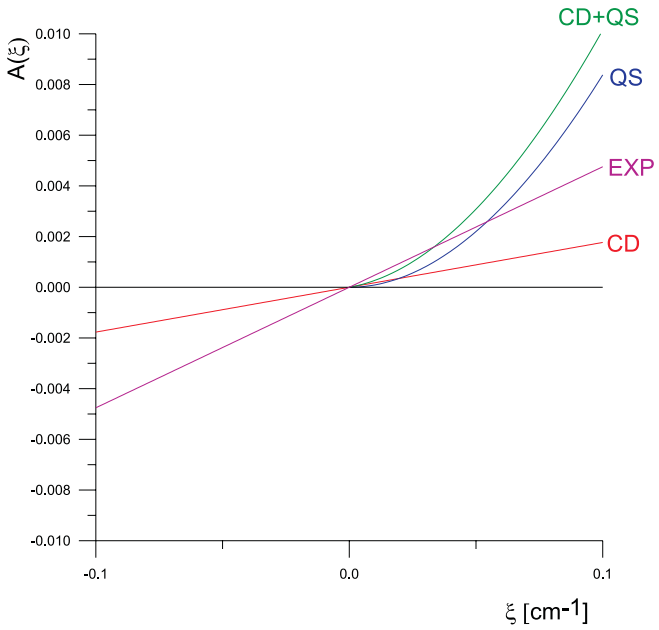

FIG. 6. (Color online) Asymmetry factors $A(\xi)$: CD, collision-time asymmetry; QS, quasistatic asymmetry; EXP, experimental values, for the 326.1-nm Cd line perturbed by neon.

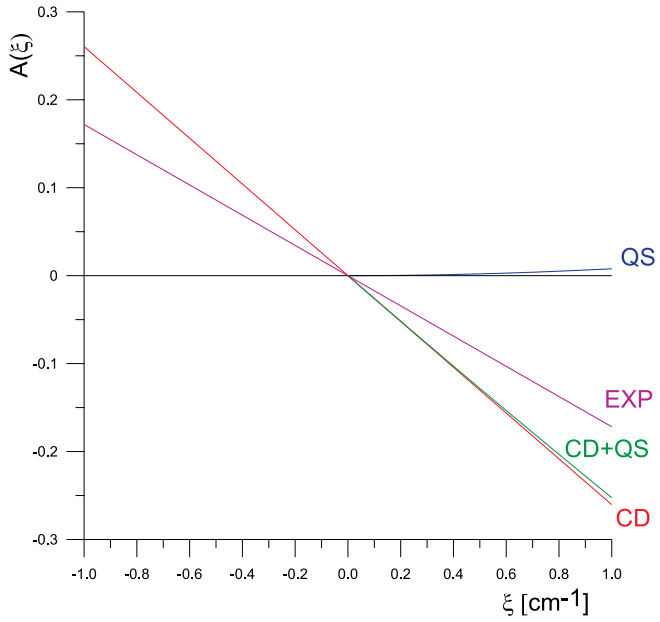

FIG. 7. (Color online) Asymmetry factors $A(\xi)$ for the 326.1-nm Cd line perturbed by xenon.

326.1-nm Cd line. The main conclusion of the present work—that the quasistatic model can explain the broadening effects caused by He and Ne on the 326.1-nm Cd line—may become a source of some controversy since it is usually believed that quasistatic theory is valid for sufficiently heavy perturbers only. Doubts about the applicability of the quasistatic model for systems of small reduced mass have been expressed in the literature many times (cf. [39]). We should note, however, that quantum-mechanical calculations performed by Herman and Sando [40] for Li-He and Na-He systems have shown that at far wings the quasistatic profile agrees with the quantum-mechanical one. Moreover, Kogan and Lisitsa [41] and Rang and Voslamber [42] have shown that even the perturbers as light as electrons in plasmas give rise to quasistatic broadening at far wings of Stark-broadened hydrogen lines. However, they are meaningful only for low-temperature plasmas and broad hydrogen lines.

As seen from Figs. 4 and 7 for heavier perturbing gases (Ar, Kr, Xe) characterized by larger values of polarizability the *quasistatic* asymmetry factors $A_{QS}(\xi)$ in the core region of the 326.1-nm Cd line are of less importance in comparison to the *collision-time* asymmetry factor $A_{CD}(\xi)$. For heavy perturbers, however, the correlation between the collisional broadening and thermal motion of the emitter may contribute significantly to the asymmetry in the core region [2,13,14,19]. On the other hand, for such perturbers the quasistatic effects are usually observed at far line wings [25,26,37].

ACKNOWLEDGMENT

This work was supported from funds for science in the years 2005–2008 as a research project (Grant No. 1P03B 065 29).

[1] R. E. Walkup, A. Spielfiedel, and D. E. Pritchard, Phys. Rev. Lett. **45**, 986 (1980); R. E. Walkup, B. Stewart, and D. E. Pritchard, Phys. Rev. A **29**, 169 (1984).
[2] M. Harris, E. L. Lewis, D. McHugh, and I. Shannon, J. Phys. B **17**, L661 (1984); **19**, 3207 (1986); I. Shannon, M. Harris, D. R. McHugh, and E. L. Lewis, *ibid.* **19**, 1409 (1986).
[3] Y. C. Chan and J. A. Gelbwachs, J. Phys. B **25**, 3601 (1992).
[4] T. Efthimiopoulos, M. E. Movsessian, and A. M. Movsessian, J. Phys. B **27**, 3017 (1994).
[5] M. V. Romalis, E. Miron, and G. D. Cates, Phys. Rev. A **56**, 4569 (1997).
[6] P. W. Anderson and J. D. Talman (unpublished); G. Traving, *Uber die Theorie der Druckverbreiterung von Spektrallinien* (Verlag G. Braun, Karlsruhe, 1960).
[7] J. Szudy and W. E. Baylis, J. Quant. Spectrosc. Radiat. Transf. **15**, 641 (1975); **17**, 681 (1977); Phys. Rep. **266**, 127 (1996).
[8] A. Royer, Acta Phys. Pol. A **54**, 805 (1978).
[9] G. Peach, Adv. Phys. **30**, 367 (1981); J. Phys. B **17**, 2599 (1984).
[10] B. N. Al.-Saqabi and G. Peach, J. Phys. B **20**, 1175 (1987).
[11] Ph. Marteau, C. Boulet, and D. Robert, J. Chem. Phys. **80**, 3632 (1984).
[12] R. Ciuryło, J. Szudy, and R. S. Trawiński, J. Quant. Spectrosc. Radiat. Transf. **57**, 551 (1997).
[13] P. R. Berman, J. Quant. Spectrosc. Radiat. Transf. **12**, 1313 (1972).
[14] J. Ward, J. Cooper, and E. W. Smith, J. Quant. Spectrosc. Radiat. Transf. **14**, 555 (1974).

[15] A. Bielski, R. Ciuryło, J. Domysławska, D. Lisak, J. Szudy, and R. S. Trawiński, Acta Phys. Pol. B **33**, 2267 (2002).
[16] A. Bielski, D. Lisak, R. S. Trawiński, and J. Szudy, Acta Phys. Pol. A **103**, 23 (2003).
[17] J. Boissoles, F. Thibault, C. Boulet, J. P. Bouanich, and J.-M. Hartmann, J. Mol. Spectrosc. **198**, 257 (1999).
[18] E. Czuchaj and H. Stoll, Chem. Phys. **248**, 1 (1999).
[19] A. Bielski, R. Ciuryło, J. Domysławska, D. Lisak, R. S. Trawiński, and J. Szudy, Phys. Rev. A **62**, 032511 (2001).
[20] A. S. Pine and J. P. Looney, J. Chem. Phys. **96**, 1704 (1992); R. Ciuryło and J. Szudy, Phys. Rev. A **63**, 042714 (2001); W. F. Wang and J. M. Sirota, J. Chem. Phys. **116**, 532 (2002); A. Predori-Cross, A. D. May, A. Vitcu, J. R. Drummond, J.-M. Hartmann, and C. Boulet, *ibid.* **120**, 10520 (2004); P.-M. Flaud, J. Orphal, C. Boulet, and J.-M. Hartmann, J. Mol. Spectrosc. **235**, 157 (2006).
[21] A. Bielski, R. Ciuryło, J. Domysławska, D. Lisak, P. Masłowski, J. Szudy, and R. S. Trawiński, Acta Phys. Pol. A **105**, 329 (2004).
[22] K. M. Sando and J. C. Wormhoudt, Phys. Rev. A **7**, 1889 (1973).
[23] N. F. Allard and J. Kielkopf, Rev. Mod. Phys. **54**, 1103 (1982).
[24] R. Beuc and V. Horvatic, J. Phys. B **25**, 1497 (1992).
[25] A. Gallagher, in *Handbook of Atomic, Molecular and Optical Physics*, edited by G. W. F. Drake (Springer Science + Business Media, New York, 2006), p. 279.
[26] G. Peach, in *Handbook of Atomic, Molecular and Optical Physics*, edited by G. W. F. Drake (Springer Science + Business Media, New York, 2006), p. 875.
[27] K. W. Ford and J. A. Wheeler, Ann. Phys. (N.Y.) **7**, 259 (1959); **7**, 287 (1959).
[28] H. M. Nussenzveig, *Diffraction Effects in Semiclassical Scattering* (Cambridge University Press, Cambridge, England, 1992).
[29] J. A. Adam, Phys. Rep. **356**, 229 (2002).
[30] I. I. Sobelman, Opt. Spektrosk. **1**, 617 (1956); I. I. Sobelman, L. A. Vainshtein, and E. A. Yukov, *Excitation of Atoms and Broadening of Spectral Lines* (Springer, Berlin, 1981).
[31] M. Baranger, Phys. Rev. **111**, 494 (1958).
[32] M. Kristensen, F. J. Blok, M. A. van Eijkelenborg, G. Nienhuis, and J. P. Woerdman, Phys. Rev. A **51**, 1085 (1995).
[33] A. Jabłoński, Phys. Rev. **68**, 78 (1945).
[34] R. Bieniek, Phys. Rev. A **15**, 1513 (1977).
[35] J. Szudy, Acta Phys. Pol. A **54**, 841 (1978).
[36] F. H. Mies, J. Chem. Phys. **48**, 482 (1968).
[37] R. E. M. Hedges, D. L. Drummond, and A. Gallagher, Phys. Rev. A **6**, 1519 (1972).
[38] W. R. Hindmarsh, A. D. Petford, and G. Smith, Proc. R. Soc. London, Ser. A **297**, 296 (1967).
[39] R. Atmad-Bitar, W. P. Lapatovich, D. Pritchard, and I. Renhorn, Phys. Rev. Lett. **39**, 1657 (1977).
[40] P. S. Herman and K. M. Sando, J. Chem. Phys. **68**, 1153 (1978).
[41] V. I. Kogan and V. C. Lisitsa, J. Quant. Spectrosc. Radiat. Transf. **12**, 881 (1972).
[42] Le Quang Rang and D. Voslamber, J. Phys. A **8**, 331 (1975).